Combining the auxin-inducible degradation system with CRISPR/Cas9-based genome editing for the conditional depletion of endogenous *Drosophila melanogaster* proteins

Melinda Bence[1], Ferenc Jankovics[1], Tamás Lukácsovich[2], Miklós Erdélyi[1]

[1]Institute of Genetics, Biological Research Centre of the Hungarian Academy of Sciences, Szeged, Hungary
[2]Brain Research Institute, University of Zürich, Zürich, Switzerland

Corresponding author
Melinda Bence
Institute of Genetics, Biological Research Centre of the Hungarian Academy of Sciences
H-6726 Szeged, Temesvari krt. 62, Hungary
Phone: +36 62 599686
E-mail: bence.melinda@brc.mta.hu

Running title
AID system in *Drosophila*

Abbreviations
AID, auxin-inducible degradation; CRISPR, clustered regularly interspaced short palindromic repeats; 2,4-D, 2,4-dichlorophenoxyacetic acid; EGFP, enhanced green fluorescent protein; FlAsH-FALI, FlAsH-mediated fluorescein-assisted light inactivation; gRNA, guide RNA; mat-tub, maternal tubulin; MCS, multi-cloning site; 1-NAA, 1-naphthylacetic acid; NGT, nanos-GAL4-tubulin; SCF, SKP1/CUL1/F-box; TEV, tobacco etch virus; TIR1, transport inhibitor response 1; UTR, untranslated region

Key words
auxin-inducible degradation, induced protein depletion, Vasa, CRISPR/Cas9, *Drosophila melanogaster*

Conflict of interest
The authors declare that they have no conflicts of interest with the content of the article.

Abstract

Inducible protein degradation techniques have considerable advantages over classical genetic approaches, which generate loss-of-function phenotypes at the gene or mRNA level. The plant-derived auxin-inducible degradation system (AID) is a promising technique which enables the degradation of target proteins tagged with the AID motif in non-plant cells. Here, we present a detailed characterization of this method employed during the adult oogenesis of *Drosophila*. Furthermore, with the help of CRISPR/Cas9-based genome editing, we improve the utility of the AID system in the conditional elimination of endogenously expressed proteins. We demonstrate that the AID system induces efficient and reversible protein depletion of maternally provided proteins both in the ovary and the early embryo. Moreover, the AID system provides a fine spatiotemporal control of protein degradation and allows for the generation of different levels of protein knockdown in a well-regulated manner. These features of the AID system enable the unravelling of the discrete phenotypes of genes with highly complex functions. We utilized this system to generate a conditional loss-of-function allele which allows for the specific degradation of the Vasa protein without affecting its alternative splice variant (*solo*) and the vasa intronic gene (*vig*). With the help of this special allele, we demonstrate that dramatic decrease of Vasa protein in the vitellarium does not influence the completion of oogenesis as well as the establishment of proper anteroposterior and dorsoventral polarity in the developing oocyte. Our study suggests that both the localization and the translation of *gurken* mRNA in the vitellarium is independent from Vasa.

Introduction

Drosophila provides a variety of experimental tools for the elimination of target proteins in order to analyze their functions in the living organism. The most frequently used techniques manipulate protein expression at the gene or mRNA level. However, the loss-of-function phenotypes generated at the gene level are irreversible. RNA interference techniques enable conditional regulation, but they act on the protein level in an indirect manner, and the ensuing effects depend on the turnover rate of the actual protein. This can be a particular problem in the case of the highly stable maternally provided proteins. In *Drosophila*, a significant level of maternally derived mRNAs and proteins are loaded into the egg, and many of them may persist throughout the whole embryogenesis. In addition, several maternal effect genes are expressed in all developmental stages and have crucial and pleiotropic functions in many key events, including oogenesis [1–5]. This further complicates their analysis, because homozygous null mutations of maternal effect genes often cause lethality or female sterility, making the examination of both their later functions and their maternal effects in the embryo impossible. Weak or temperature-sensitive alleles can overcome these limitations, however, they are not always available for a given gene. In addition, mutant alleles often affect more splice variants, which makes the investigation of specific phenotypes more confounding.

Recently, a variety of methods have been developed that are able to induce direct and specific protein degradation. Some of them, such as the TEV protease-mediated cleavage or the GFP-nanobody-directed degradation [6,7], have been adapted to *Drosophila*. These methods provide conditional protein depletion that can be regulated by the tissue-specific expression of the TEV protease or the GFP-nanobody. Other methods such as photo-inactivation by FlAsH-FALI or the temperature-sensitive intein enable a more defined spatiotemporal protein depletion [8,9]. However, both the reactive oxygen species generated by FlAsH-FALI and the elevated temperature can result in unwanted physiological changes and off-target effects.

The plant-derived auxin-inducible degradation (AID) system is a promising technique to induce rapid and reversible protein depletion [10]. This method is based on the ability of the plant F-box protein TIR1 to incorporate into the highly conserved SKP1/CUL1/F-box (SCF) ubiquitin ligase complex in non-plant cells. Therefore, the heterologously expressed plant TIR1 protein is able to induce the polyubiquitination and proteasomal degradation of target proteins tagged with the auxin-inducible degron (AID) motif. The TIR1 protein binds to the AID motif exclusively in the presence of the auxin hormone. Auxin is a cell-permeable small

molecule and can easily penetrate into cells, which provides an excellent possibility for temporal control of protein degradation. The AID system was first applied in yeast and in cultured vertebrate cell lines [10–12]. Subsequently, *Caenorhabditis elegans* was used to show that this technique can be adapted to intact multicellular organisms as well [13]. A most recent study on *Drosophila melanogaster* demonstrated that the AID system is able to induce protein degradation in somatic cells during the larval stages without significant side effects [14].

Here, we present a detailed characterization of the AID system employed during the adult oogenesis of *Drosophila*. We applied this method to deplete Nanos and Vasa, two well-known and highly pleiotropic maternal effect proteins. We show that auxin administration or TIR1 overexpression in the germline does not influence the viability and fertility of adult flies and has no harmful maternal effects. The AID system enables rapid and reversible protein degradation in the ovary, and the maternally loaded TIR1 and auxin can be functional in the early embryo as well. Furthermore, we demonstrate that the combination of the AID system with the CRISPR/Cas9-based genome editing techniques enables the complete elimination of endogenously expressed proteins.

Results

The AID system is able to induce reversible protein degradation in the early embryo of Drosophila melanogaster

To examine whether the plant-derived AID system can be functional during early embryogenesis, we established a fly line expressing an AID-tagged dominant negative form of the Nanos protein (AID:nos-bcd3'UTR). In this fly line, the localization signal of *nanos* mRNA was replaced by a localization and translational signal derived from the *bicoid* 3'UTR. These flies lay eggs in which the transgenic Nanos protein is mislocalized to the anterior pole, resulting in embryos with a bicaudal phenotype (Figure 1B) [15]. To introduce the AID system into this fly line, the AID motif was fused N-terminally to the transgenic Nanos. We used the minimal size AID motif, as it has been shown that this region itself induces more efficient protein degradation than the full-length degron [12]. The 9xMyc-tagged TIR1 protein was expressed in the female germline under the control of UASp promoter and nosGal4VP16 driver. Auxin administration was achieved by feeding the flies with a paste prepared by dissolving inactive yeast extract in 1M auxin solution. Neither TIR1 overexpression nor auxin treatment caused lethal effects in the adult flies. One day old, completely developed embryos of the *AID:nos-bcd3'UTR; nosGal4VP16>UASpTIR1* transgenic females were analyzed by cuticle preparation. Upon auxin administration, the dominant-negative bicaudal phenotype was suppressed, indicating that the AID system was able to degrade the AID-tagged mislocalized Nanos protein (Figure 1C). Suppression of the bicaudal phenotype appeared already at the first day of auxin treatment, and its penetrance increased constitutively with time, reaching the maximum on the third day. (Figure 1D). One day after auxin removal, the suppression decreased, and after two days no suppressed bicaudal phenotype was detected, demonstrating that the AID system acts in a reversible manner. Auxin treatment did not influence the proportion of undeveloped embryos indicating that auxin has no harmful maternal effects (Figure 1D).

Endogenous Vasa protein can be conditionally depleted by the genomic insertion of the AID motif sequence

In order to investigate the effectiveness of the AID system in degrading endogenously expressed proteins, we applied CRISPR/Cas9-based homologous recombination for the insertion of the AID motif into the genome. The *vasa* gene was selected for this procedure as

its functions and expression pattern are well known [16]. The Vasa protein is expressed in the germline throughout all stages of development. It is required for the completion of oogenesis, and the maternally loaded Vasa protein has an essential role in embryonic patterning and germ cell specification. Therefore, its loss-of-function phenotypes, such as oogenesis defects during adulthood or lack of abdominal segments and pole cells in the early embryo, can be easily detected.

We introduced the minimal size AID motif sequence right before the stop codon of the *vasa* gene (Figure 2). In addition to the AID motif, an EGFP tag was also inserted to enable the direct visualization of the Vasa protein. The AID:EGFP tagged *vasa* gene was fully functional since in homozygous condition it resulted in a wild-type, viable and fertile phenotype. Expression and subcellular localization of the tagged Vasa protein in the adult ovary and in the early embryo was identical with that of the wild-type (Figure 3).

To induce Vasa degradation, we expressed the TIR1 protein in the germline of flies homozygous for *vasa:AID:EGFP* using various maternal Gal4 sources (*mat-tub-Gal4*, *NGT-Gal4*, *nosGal4VP16*). Flies were fed with 1M auxin for three days, and their ovaries were dissected to analyze Vasa and TIR1 protein expression by confocal microscopy. The level of the Vasa protein drastically decreased in the ovaries in all of the investigated fly lines. The Vasa protein was specifically absent only where the TIR1 protein was expressed, indicating that the pattern of degradation correlates well with TIR1 localization (Figure 4). Accordingly, in the ovaries of *vasa:AID:EGFP; mat-tub-Gal4>UASpTIR1* females, we observed Vasa depletion starting from stage 2 egg chambers. Consistently, the TIR1 protein was expressed throughout oogenesis, except in the germarium (Figure 4A). In the *vasa:AID:EGFP; NGT-Gal4>UASpTIR1* females, the Vasa protein was absent in the later stages of oogenesis starting from stage 9, and we found partial Vasa degradation in the germarium as well. The TIR1 protein localization again showed a similar pattern to Vasa depletion (Figure 4B). In the ovaries of *vasa:AID:EGFP; nosGal4VP16>UASpTIR1* females, Vasa depletion started from oogenesis stage 9. In parallel, the TIR1 protein was expressed at a higher intensity in the later-stage egg chambers (Figure 4C). To check the reversibility of the system, ovaries were analyzed two days after auxin removal, and we found that Vasa protein expression completely reappeared (Figure 4D).

To confirm these results, the Vasa protein in ovaries of *vasa:AID:EGFP; nosGal4VP16>UASpTIR1* females were further examined by Western blot analysis. After three days of auxin treatment, we found a dramatic decrease of Vasa protein levels in the ovaries. The small amount of residual protein is most likely due to the undegraded Vasa

expressed in the germarium and in early-stage egg chambers. Two days after auxin withdrawal, Vasa protein expression was fully restored (Figure 5).

Vasa depletion by the AID system efficiently generates loss-of-function phenotypes

As shown in Figure 4, Vasa depletion, detected in all of the investigated fly lines, did not influence the completion of oogenesis, and the ovaries were similar to the wild-type. This allowed us to examine the maternal effects of Vasa degradation on the laid embryos. Interestingly, the embryonic phenotypes were similar regardless of which Gal4 source was applied. In all cases, the vast majority of laid eggs failed to hatch. Cuticle preparations revealed that these embryos lack abdominal segments, showing a typical posterior phenotype caused by many hypomorphic *vasa* alleles (Figure 6) [1]. The anteroposterior and dorsoventral polarity of the oocytes developed normally, as we never observed eggs with a posterior micropyle or with fused or lacking dorsal appendages. Proper polarity was further confirmed by immunostaining of the Gurken protein in the ovary of auxin-treated *vasa:AID:EGFP; mat-tub-Gal4>UASpTIR1* females. Gurken is the major determinant of oocyte polarity both along the anteroposterior and the dorsoventral axes [17,18]. We found that Gurken is expressed at the posterior pole of the egg chambers during early oogenesis, and it is subsequently localized to the dorsal-anterior corner of the oocyte, showing a typical wild-type expression pattern (Figure 7).

To explore the dynamics of auxin-induced protein degradation, embryos laid by the *vasa:AID:EGFP; nosGal4VP16>UASpTIR1* females were further investigated over the course of time. Adult females were fed with 1M auxin for four days and their laid eggs were analyzed by cuticle preparations. Already on the first day, auxin treatment induced depletion of Vasa, as indicated by the appearance of embryos with abdominal defects. On the third day of auxin treatment, the posterior phenotype reached maximal penetrance, and only a few hatched larvae (1.94 %) were detected. The depletion was fully reversible, as indicated by the complete restoration of wild-type abdominal patterning after auxin withdrawal (Figure 8A). Consistently with the embryonic phenotypes, Western blot analysis revealed significant Vasa depletion in the laid eggs upon auxin treatment. Vasa protein reappeared one day after the auxin withdrawal and its level completely restored on the second day (Figure 8C). In the control experiment, we used *vasa:AID:EGFP; UASpTIR1* flies without any Gal4 source to prevent TIR1 expression. In these flies, auxin treatment caused no substantial abdominal defect (Figure 8B). This result indicates that the observed posterior patterning defect is a direct consequence of the TIR1-mediated Vasa depletion and is not due to a side effect of the

auxin treatment. Furthermore, our results demonstrated that 1M auxin has no harmful maternal effects, as the percentage of undeveloped embryos did not change during the treatment (Figure 8A,B).

The penetrance and expressivity of loss-of-function vasa phenotypes correlate with auxin concentration

We next investigated whether the efficiency of protein depletion depend on the level of auxin. For this purpose, *vasa:AID:EGFP; nosGal4VP16>UASpTIR1* flies were fed with increasing concentrations of auxin, and their progeny were analyzed. As shown in Figure 9A, the penetrance of the abdominal defects was directly proportional to the applied auxin concentration. Maximum penetrance was achieved by using 0.5-2 M auxin solution. Higher levels of auxin were less effective and possibly toxic, as the number of undeveloped embryos increased. Vasa degradation in the laid embryos was followed by Western blot which further supported that the efficiency of depletion correlates with the applied auxin concentration (Figure 9B).

Vasa protein determines maternal phenotypes in a dose-dependent manner, as the moderate reduction in the amount of maternally provided Vasa results in sterility, whereas further reduction leads to abdominal defects. For example, females homozygous for the temperature sensitive vas^{O14} allele, at the restrictive temperature, produce viable progeny that show proper segmentation, but still lack germ cells [19]. Therefore, we checked the fertility of the viable progeny of females fed with lower concentrations of auxin (25-250 mM). The hatched larvae were allowed to develop until adulthood, and then their gonads were examined. We found that the majority (50-60%) of ovaries and testes were agametic showing a typical germ cell-less phenotype (Figure 10). These findings indicate that increasing the auxin concentration results in gradual protein depletion, which enables the generation of a phenotypic series. In this manner, we were able to find the threshold level of Vasa necessary for embryonic patterning but insufficient for germ cell formation.

Auxin analogues are able to activate the AID system in Drosophila melanogaster

It has been reported that synthetic auxin analogues 1-naphthaleneacetic acid (1-NAA) and 2,4-dichlorophenoxyacetic acid (2.4-D) are able to activate the AID system in plants, however, they have a lower affinity to the TIR1 receptor [20,21]. Consistent with this result, we found that both analogues were able to induce Vasa depletion in *vasa:AID:EGFP; nosGal4VP16>UASpTIR1* females, as indicated by the appearance of embryos with

abdominal defects (Figure 11). 1-NAA acted with a similar efficiency as auxin, whereas treatment with 2.4-D was less effective. This finding further demonstrates that the observed abdominal defect is not an aspecific effect of auxin since its synthetic analogues induce the same phenotype. Moreover, our result revealed that the minimal size AID motif used in this study retained the ability to activate the AID system by auxin analogues as well.

Discussion

In the present study, we demonstrated that the plant-derived AID system can be efficiently employed in the female germline of *Drosophila melanogaster*. We showed that the small size of the AID motif enables highly efficient genomic integration by the CRISPR/Cas9-based technology. Insertion of the degron did not affect protein expression, localization, and the degron-tagged proteins were fully functional. Auxin can be easily administered by feeding, and in an optimal, effective concentration it has no adverse effects on the adult flies. Finally, adult flies expressing the TIR1 protein in their germline are viable and fertile.

Our study involved two maternal genes to analyze the features of auxin-induced protein degradation in the ovary and in the early embryo. The *vasa* gene is expressed throughout oogenesis, and its protein is loaded directly into the egg, whereas the product of the *nanos-bcd3'UTR* transgene is transferred into the oocyte as mRNA and translated only after fertilization [22,15]. The AID system was able to induce complete Vasa degradation at distinct stages of oogenesis, leading to a total lack of Vasa protein in the embryos. Depletion of the mislocalized Nanos demonstrated that the AID system is also active during the early embryonic stages. This result indicates that the TIR1 protein and auxin can be transported into the mature oocyte, allowing the AID system to induce protein degradation in the laid embryo. However, rescue of the bicaudal phenotype was only partial, as we could not detect normally segmented, viable larvae even after treatment with higher auxin concentrations (data not shown). This observation suggests that depletion of the mislocalized Nanos protein was incomplete. It may be due to the instability of the TIR1 protein or auxin, which results in lower concentrations in the laid embryo compared to the ovary, where the supply of these components is continuous. Staller MV et al. also found that maternally loaded shRNAs are less effective in the early embryo than they act directly in the ovary [5]. Another explanation of the partial rescue could be that the translation of the transgene is highly effective, and the action of mislocalized Nanos protein is faster than its degradation rate by the AID system. This hypothesis is supported by the fact that the anteriorly localized, ectopic Nanos possesses greater activity and induces abdomen formation in a lower concentration than localized posteriorly [15].

The dynamics of the AID system was similar for both proteins. The maternal effect of protein degradation appeared already after the first day of auxin treatment. This result indicates that the accumulation of auxin in the ovary takes less than one day. The egg chambers are permeable to auxin probably until the chorion wraps the mature oocyte. This occurs during

stages 13-14 and takes approximately three hours, which is only a short interval of the eight-day-long adult oogenesis [23,24]. Presumably, auxin activates the AID system rapidly upon passing into the egg chambers, since in other model systems the target proteins were depleted as fast as 20-30 minutes, and a complete loss of the protein was observed within 1 hour in *Drosophila* S2R+ cells [11−14]. In adult flies, recovery occurred rapidly within one day after auxin withdrawal, indicating that the elimination of auxin from the ovary is also highly efficient. Consequently, these features allow rapid manipulation of protein levels by the AID system over a long period of oocyte development.

Direct insertion of the AID motif into the genomic *vasa* locus enabled us to regulate the level of the endogenously expressed Vasa protein. Classical loss-of-function *vasa* alleles can affect the function and expression of other proteins since the alternative splice variant of *vasa*, the sisters-on-the-loose (*solo*) and the vasa intronic gene (*vig*), are also located in the same locus [25,26]. This complicates investigation of the specific role of the Vasa protein itself. Moreover, as Vasa is expressed throughout development, its adult phenotypes are influenced by earlier effects. Our AID-tagged *vasa* allele allowed us to examine specific *vasa* phenotypes during adult oogenesis.

Various maternal Gal4 sources were tested for the expression of the TIR1 protein in the female germline. The pattern of Vasa depletion in the ovary correlated well with TIR1 localization, demonstrating that the AID system is able to achieve a fine spatial control of protein destruction. The phenotypes obtained by the AID system were similar to those of hypomorphic *vasa* mutants: the flies did not exhibit any defects in oogenesis, and they laid numerous eggs. This result is not surprising, since none of the used Gal4 sources drove TIR1 expression in all stages of oogenesis. However, Vasa depletion lead to maternal-effect lethality in all cases, since the laid embryos were not viable and failed to hatch. Embryonic lethality was caused exclusively by abdominal defects, as the dorsoventral axis of the embryos developed normally. All of these phenotypes highly resemble those observed in *vas[1]* mutants. In *vas[1]* mutant females, the Vasa protein is expressed at the wild-type level in the germarium and in the early-stage egg chambers, but is absent later in oogenesis [19,22]. Our experiment using the *mat-tub-Gal4* driver provides further evidence that Vasa expression in the germarium is sufficient for the completion of oogenesis, as well as for the establishment of dorsoventral polarity. Contrarily, in *vasa*-null ovaries, most of the egg chambers degenerate during the early vitellogenic stages, and the few laid eggs are strongly ventralized [27,28]. Therefore, it seems reasonable to speculate that the key events of oogenesis regulated by Vasa are restricted to the germarium. However, in the case of *vasa*-null alleles, we cannot exclude

that earlier developmental events interfere with the adult phenotypes. Furthermore, we found that the significant reduction in the level of Vasa in the germarium induced by the *NGT-Gal4* driver did not increase the severity of phenotypes even after ten days of auxin treatment. This result implies that only a small amount of Vasa protein is sufficient in the germarium for oocyte development. Consistently, even vas^{LYG2} homozygotes are able to complete oogenesis though the level of Vasa in their ovaries is only about 2% of the wild-type level [28].

Polarity defects observed in the *vasa*-null and strong hypomorphic *vasa* ovaries were explained by the greatly reduced level of the Gurken protein [28,29]. Furthermore, mutations in the *vasa* alleles that affect the DEAD-box RNA helicase domain or reduce binding to the translation initiation factor eIF5B prevent the accumulation of Gurken in the ovary [30,31]. These results imply that Vasa has a crucial role in the translation of *gurken* mRNA. Moreover, Tinker et al suggest that Vasa is also necessary for the proper localization of *gurken* mRNA [32]. Gurken is responsible for the establishment of the anteroposterior axis of the egg chamber during the early stages, and it subsequently specifies the dorsoventral axis of the oocyte during mid-oogenesis [17,18]. In contrast, we found that the anteroposterior polarity is maintained and the dorsoventral axis also develops properly even when Vasa is expressed only in the germarium. Consistently, the Gurken protein accumulated and localized as in the wild-type ovary. Our results are in agreement with a previous study suggesting that the translation of *gurken* is independent from Vasa during the later stages of oogenesis [29]. Alternatively, Vasa depletion was incomplete and a trace amount of Vasa remained in the vitellarium which was sufficient for Gurken translation. However we observed proper Gurken accumulation even after the Vasa level was further decreased by removing one copy of *vasa* (data not shown).

The maternally loaded Vasa protein has an essential role in pole plasm assembly, which is responsible for germ cell specification as well as for somatic posterior patterning during early embryogenesis [1,22,19]. Accordingly, AID-induced Vasa depletion caused strong abdominal defects in the laid embryos. The severity of this phenotype was independent of whether Vasa was depleted only in the older egg chambers or it was already absent during the earlier stages as well because both cases resulted in a complete lack of abdomen. This indicates that Vasa expression in later-stage egg chambers is sufficient for the proper segmentation of the embryo. However, when the auxin concentration was reduced, the penetrance of embryos with abdominal defects decreased. Moreover, lower auxin concentrations resulted in less severe phenotypes ranging from the appearance of a few abdominal segments to normally developed and hatched embryos. Further investigations revealed that the vast majority of the

viable progeny were sterile, indicating that despite proper somatic segmentation, the development of germ cells was abolished in many cases. Consistently, it has been suggested previously that the threshold level of Vasa necessary for the determination of the posterior soma is less than that necessary to induce pole cell formation [28]. Taken together, we conclude that the efficiency of Vasa degradation correlates with the applied auxin concentration. Consequently, auxin not only provides temporal control, but by altering its concentration, we can achieve distinct phenotypes and various degrees of penetrance.

In summary, we have established a novel tool which enables precise analysis of adult and early embryonic phenotypes of maternal genes in *Drosophila melanogaster*. The AID system provides a fine spatiotemporal control of protein depletion and is able to generate different levels of protein knockdown in a well-regulated manner. All of these features make the AID system suitable for the investigation of pleiotropic proteins such as Vasa. The versatility of this method is enhanced by the rapidly developing genome editing and fosmid-based techniques that allow efficient insertion of the AID motif into any *Drosophila* protein [33,34] Moreover, a previous study demonstrated that this technique efficiently degrades proteins in somatic cells and works in larval stages as well, suggesting that the AID system can be a valuable tool in all fields of *Drosophila* genetics.

Materials and Methods

Drosophila strains

ΦC31X; attP 86Fa (#24486), *ΦC31X; attP 58A* (#24484), *vas-Cas9* (#51324), w[1118]; Df(2L)BSC299/CyO (#23683); Oregon-R (#5); maternal Gal4 drivers: *w[1118]; P{GAL4::VP16-nos.UTR}CG6325[MVD1]* (nosGal4VP16) (#4937), *w*; PenD14/CyO; P{GAL4-nos.NGT}9/TM6B, Tb+* (NGT-Gal4) (#25394), *w*; P{matα4-GAL-VP16}V37* (mat-tub-Gal4) (#7063) were obtained from the Bloomington Stock Center.

Plasmid construction and transgenesis

To generate the *AID:nos-bcd3'UTR* transgenic fly line, the pAttB-nos5'-AIDnosCDS-bcd_nos3' plasmid was created via the following consecutive cloning steps. First, a Multi-Cloning Site (MCS) was inserted between the HindIII (at position 4855) and SpeI (at position 5986, after partial SpeI digestion due to another downstream SpeI site) sites of the pUAST-AttB vector (Bischof et al. 2007, Genebank accession #: EF362409) on a synthetic double-stranded oligonucleotide. By this insertion, the MCS replaced the UAS and SV40T sequences but left the AttB donor site in place. The separate components of the expression cassette were PCR-amplified from *Drosophila* genomic DNA template using the following primers; restriction sites are underlined: *Nanos* promoter: 5'-A<u>AA GCT TCG</u> ACC GTT TTA ACC TCG-3' sense and 5'-G<u>GA ATT C</u>AA CAT GGC GAA AAT CCG GGT CG-3' antisense primer. *Nanos* gene: 5'-A<u>AG ATC T</u>TC CGC AGC AAC TTG GAG GGC AG-3' sense and 5'-T<u>AC GCG T</u>CT AAA CCT TCA TCT GTT GCT TG-3' antisense primer. *Bicoid* 3'UTR (does not contain the nos response element): 5'-T<u>AC GCG T</u>AG AAA GTT AGG TCT AGT C-3' sense and 5'-A<u>CT CGA G</u>GC CTA ACA GAT TGC AAT GCT C-3' antisense primer. *Nanos* polyA: 5'-G<u>CT CGA G</u>TG CCA AAT AAA GAA ATG G-3' sense and 5'-C<u>TC TAG A</u>GA ACG CTT CCG GAC GTA GAG-3' antisense primer. The auxin-inducible degron (AID) sequence was PCR-amplified from the pSM409 plasmid (gift from Helle D. Ulrich) containing the 44-amino acid minimal degron derived from the Arabidopsis thaliana IAA17 protein [12]. For amplification, the following oligos were used: 5'-T<u>GA ATT C</u>CA TGC CTA AAG ATC CAG CCA AAC CTC-3' sense and 5'-A<u>AG ATC T</u>TC ACG AAC GCC GCC GCC TCC-3' antisense primers. The PCR products were digested with restriction enzymes and subcloned into the TopoTA PCR cloning vector (Thermo Fisher Scientific). The components were then transferred one by one from the TopoTA subclones into the MCS in

the following order: nos5' by HindIII-EcoRI double digestion, AID sequence with EcoRI-BglII, bcd 3'UTR with MluI-XhoI, nos polyA by XhoI-XbaI and finally, the nos genomic gene by BglII-MluI. The pAttB-nos5'-AIDnosCDS-bcd-nos3' plasmid was integrated at the attP58A3 landing site.

For the TIR1 expression construct, the *OsTIR1-9xMyc* sequence was PCR-amplified from the pNHK53 plasmid (NBRP-Yeast, BYP6744) using 5'-AAA <u>GGT ACC</u> GCC ACC ATG ACG TAC TTC CCG GAG GA-3' sense (where the KpnI site is underlined) and 5'-AAA <u>GGA TCC</u> TTA GCT AGT GGA TCC GTT CAA GTC-3' antisense (where the BamHI site is underlined) primers. The PCR product was digested with KpnI and BamHI restriction enzymes and cloned into the pUASp-K10attB vector. The pUASp-K10attB vector enabling germline-specific gene expression was a kind gift from Beat Suter [35]. The construct was integrated into the genome at the attP58A3 and attP86E18 landing sites.

Tagging via the CRISPR/Cas9-based technology

To search for guide RNA target sites near the C-terminal end of the *vasa* gene, the flyCRISPR Optimal Target Finder website (http://tools.flycrispr.molbio.wisc.edu/targetFinder) was used. Two guide RNA recognition sites, located in the last intron: 5'-GCGTGGCAGGGTGAGTAAAC<u>TGG</u>-3' and downstream of the vasa 3'UTR in intergenic region: 5'-<u>CCC</u>AACTAATACCGTGTACTATC-3' (the PAM sequences are underlined), were selected. The target site sequences were cloned into the pU6-BbsI-chiRNA plasmid (Addgene, #45946) [36] with the following oligos: 5'-CTT CGC GTG GCA GGG TGA GTA AAC-3' sense and 5'-AAA CGT TTA CTC ACC CTG CCA CGC-3' antisense oligos for cloning the intronic target site; 5'-CTT CGA TAG TAC ACG GTA TTA GTT-3' sense and 5'-AAA CAA CTA ATA CCG TGT ACT ATC-3' antisense oligos for cloning the intergenic target site. The cleavage efficiency of guide RNAs was tested in the *vas>Cas9* line by embryonic PCR according to the protocol on the http://flycrispr.molbio.wisc.edu/protocols/embryonicPCR website. The expected 425 bp deletion produced by the guide RNA pair was clearly demonstrated by gel electrophoresis.

For construction of the repair template, homology sequences were PCR-amplified from genomic DNA of the *w^1118* fly strain. PCR products were cloned into the pSM409 C-terminal tagging plasmid (gift from Helle D. Ulrich) harbouring the minimal truncated form of the AID sequence fused to EGFP tag [12]. The 1550 bp genomic fragment right before the stop codon was cloned using the 5'-AAA A<u>CA GCT G</u>AC AAC ATA CCG TT AAG GTA ACA A-3' sense (PvuII site is underlined) and 5'- AAA <u>GTC GAC</u> ATC CCA TTG CTC TTC TTC CT-

3' antisense (SalI site is underlined) primers. After digestion with PvuII and SalI, the PCR product was cloned into the pSM409 plasmid upstream of the AID-EGFP tag. The 1730 bp genomic fragment right after the stop codon was PCR-amplified with the 5'- AAA <u>GGC GCG CC</u>A ATG TAT GGA CAT AGA TTT C-3' sense (AscI site is underlined) and 5'- AAA <u>GAG CTC</u> AAT TTG GCA CTC ACC ATT CT-3' antisense (SacI site is underlined) primers. The PCR product was digested with AscI and SacI enzymes and cloned into the pSM409 plasmid downstream of the AID-EGFP tag.

To prevent cutting of the repair template, guide RNA recognition sites were eliminated on the plasmid using a site-directed mutagenesis kit (Agilent Technologies, #210518). The following mutagenic primers were applied to mutate the intronic target site (mutated nucleotides are emboldened): 5'-GTG CGT GGC AGG GTG AGT AAA **GTC C**AA AAA CTT CTT TTG TTT TGC AC-3' sense and 5'-GTG CAA AAC AAA AGA AGT TTT T**GG A**CT TTA CTC ACC CTG CCA CGC AC-3' antisense primers. The intergenic target site was mutated to create NheI and XhoI restriction sites to aid further cloning of the DsRed marker gene. The following mutagenic primers were used (mutated nucleotides are emboldened; NheI site is double underlined; XhoI site is underlined): 5'-GTT GCA AAA CTT AAC AGA AAC GTG CAC TTT GAT <u><u>GCT AGC</u></u> TAA T**CT CGA** GTA CTA TCA TGT GTT TGG TTT TAA GTA CTC ATC-3' sense and 5'-GAT GAG TAC TTA AAA CCA AAC ACA TGA TAG TAC **T**C<u>G AG</u>A TTA <u><u>GC</u>T <u>AGC</u></u> ATC AAA GTG CAC GTT TCT GTT AAG TTT TGC AAC-3' antisense primers.

3xP3 DsRed cassettes flanked by loxP sites were excised from the pHD-DsRed plasmid (Addgene #51434) [37] with XhoI and NheI digestion and subcloned into the repair template plasmid.

The pU6-BbsI-chiRNA plasmids (250-250 ng/µl) and the repair template plasmid (500 ng/µl) were mixed and injected into embryos of the *vas>Cas9* fly line. The progeny of injected flies were screened for eye-specific expression of the DsRed marker gene. Proper integration of the repair template was confirmed by sequencing.

Cuticle preparation

Embryos were collected 24 hours after egg laying and dechorionated by rinsing with 50% bleach. Dechorionated embryos were then mounted in 1:1 mixture of Hoyer's medium and lactic acid and incubated at 60°C overnight.

Western blot

For western blot analysis, ovaries were dissected from 4- and 6-day-old females. 0-2-hour-old embryos were dechorionated by rinsing with 50% bleach. Samples were homogenized by sonication in Laemmli buffer (50 mM Tris-HCl pH6.8, 2% SDS, 0.1 % bromphenol blue, 10% glycerol, 100 mM 2-mercaptoethanol, supplemented with complete protease inhibitor cocktail (Roche, #10481900) and heat denatured (100°C, 5 min). Proteins were electrophoresed on 10% SDS-polyacrylamide gel and subsequently transferred onto PVDF membrane (Millipore) for immunoblotting. Membranes were incubated in rabbit anti-GFP (1:6000, Life Technologies) or mouse anti-β-tubulin (1:300, DSHB) primary antibodies at 4 °C overnight. Secondary antibodies were HRP-conjugated anti-rabbit IgG (1:10000, Sigma) or HRP-conjugated anti-mouse IgG (1:6000, Sigma) antibodies. Immunocomplexes were visualized by enhanced chemiluminescence reaction (Millipore).

Immunostaining

Ovaries were dissected from 4-day-old females and fixed in PBS with 4% formaldehyde for 20 min. Early embryos (0-60 min) were dechorionated in 50% bleach and fixed for 30 min in 1:1 mixture of heptane and 4% formaldehyde. Subsequently, embryos were devitellinized in 1:1 mixture of methanol/heptan solution by vigorous shaking. The samples were incubated with mouse anti-c-myc (1:100, Santa Cruz Biotechnology), mouse anti-Gurken (1:10, 1D12, DSHB) or goat anti-Vasa (1:100, Santa Cruz Biotechnology) primary antibody at 4 °C overnight. Anti-mouse Alexa Fluor 546 (1:600, Life Technologies) and anti-goat Alexa Fluor 546 (1:600, Life Technologies) were used as secondary antibody, and DAPI (200 ng/ml, Sigma) was also applied. Stained ovaries and embryos were mounted in Fluoromount-G medium (SouthernBiotech, #0100-01). All micrographs were taken using a Leica SP5 confocal laser scanning microscope.

Treatment with auxin and auxin analogues

Ten female and five male flies were placed in egg laying vials containing apple juice agar. 100 µl auxin (Sigma, I5148), 1-naphthylacetic acid (1-NAA) (Sigma, #N0640), or 2,4-dichlorophenoxyacetic acid 2,4 (2,4-D) (Sigma, #D7299) dissolved in water (0.025-4M) were mixed with 500 mg inactive yeast extract (Molar Chemicals). The yeast paste was spotted onto the wall of the vial. Flies were transferred into new vials with fresh yeast paste every day and kept at 25 °C in the dark.

Acknowledgments

Author Contributions

MB, FJ and ME conceived the project, designed the experiments and wrote the manuscript. MB and FJ performed the experiments and analyzed the data. TL generated the *AID:nos-bcd3'UTR* plasmid.

References

1 Schüpbach T & Wieschaus E (1986) Maternal-effect mutations altering the anterior-posterior pattern of the Drosophila embryo. *Rouxs Arch. Dev. Biol.* **195**, 302–317.

2 Schüpbach T & Wieschaus E (1989) Female sterile mutations on the second chromosome of Drosophila melanogaster. I. Maternal effect mutations. *Genetics* **121**, 101–117.

3 Schüpbach T & Wieschaus E (1991) Female sterile mutations on the second chromosome of Drosophila melanogaster. II. Mutations blocking oogenesis or altering egg morphology. *Genetics* **129**, 1119–1136.

4 Yatsu J, Hayashi M, Mukai M, Arita K, Shigenobu S & Kobayashi S (2008) Maternal RNAs encoding transcription factors for germline-specific gene expression in Drosophila embryos. *Int. J. Dev. Biol.* **52**, 913–923.

5 Staller MV, Yan D, Randklev S, Bragdon MD, Wunderlich ZB, Tao R, Perkins LA, Depace AH & Perrimon N (2013) Depleting gene activities in early Drosophila embryos with the "maternal-Gal4-shRNA" system. *Genetics* **193**, 51–61.

6 Harder B, Schomburg A, Pflanz R, Küstner K, Gerlach N & Schuh R (2008) TEV protease-mediated cleavage in Drosophila as a tool to analyze protein functions in living organisms. *BioTechniques* **44**, 765–772.

7 Caussinus E, Kanca O & Affolter M (2012) Fluorescent fusion protein knockout mediated by anti-GFP nanobody. *Nat. Struct. Mol. Biol.* **19**, 117–121.

8 Zeidler MP, Tan C, Bellaiche Y, Cherry S, Häder S, Gayko U & Perrimon N (2004) Temperature-sensitive control of protein activity by conditionally splicing inteins. *Nat. Biotechnol.* **22**, 871–876.

9 Venken KJT, Kasprowicz J, Kuenen S, Yan J, Hassan BA & Verstreken P (2008) Recombineering-mediated tagging of Drosophila genomic constructs for in vivo localization and acute protein inactivation. *Nucleic Acids Res.* **36**, e114.

10 Nishimura K, Fukagawa T, Takisawa H, Kakimoto T & Kanemaki M (2009) An auxin-based degron system for the rapid depletion of proteins in nonplant cells. *Nat. Methods* **6**, 917–922.

11 Holland AJ, Fachinetti D, Han JS & Cleveland DW (2012) Inducible, reversible system for the rapid and complete degradation of proteins in mammalian cells. *Proc. Natl. Acad. Sci. U. S. A.* **109**, E3350-3357.

12 Morawska M & Ulrich HD (2013) An expanded tool kit for the auxin-inducible degron system in budding yeast. *Yeast Chichester Engl.* **30**, 341–351.

13 Zhang L, Ward JD, Cheng Z & Dernburg AF (2015) The auxin-inducible degradation (AID) system enables versatile conditional protein depletion in C. elegans. *Dev. Camb. Engl.* **142**, 4374–4384.

14 Trost M, Blattner AC & Lehner CF (2016) Regulated protein depletion by the auxin-inducible degradation system in Drosophila melanogaster. *Fly (Austin)*, 1–12.

15 Gavis ER & Lehmann R (1992) Localization of nanos RNA controls embryonic polarity. *Cell* **71**, 301–313.

16 Lasko P (2013) The DEAD-box helicase Vasa: evidence for a multiplicity of functions in RNA processes and developmental biology. *Biochim. Biophys. Acta* **1829**, 810–816.

17 González-Reyes A, Elliott H & St Johnston D (1995) Polarization of both major body axes in Drosophila by gurken-torpedo signalling. *Nature* **375**, 654–658.

18 Roth S, Neuman-Silberberg FS, Barcelo G & Schüpbach T (1995) cornichon and the EGF receptor signaling process are necessary for both anterior-posterior and dorsal-ventral pattern formation in Drosophila. *Cell* **81**, 967–978.

19 Lasko PF & Ashburner M (1990) Posterior localization of vasa protein correlates with, but is not sufficient for, pole cell development. *Genes Dev.* **4**, 905–921.

20 Dharmasiri N, Dharmasiri S & Estelle M (2005) The F-box protein TIR1 is an auxin receptor. *Nature* **435**, 441–445.

21 Teale WD, Paponov IA & Palme K (2006) Auxin in action: signalling, transport and the control of plant growth and development. *Nat. Rev. Mol. Cell Biol.* **7**, 847–859.

22 Hay B, Jan LY & Jan YN (1990) Localization of vasa, a component of Drosophila polar granules, in maternal-effect mutants that alter embryonic anteroposterior polarity. *Dev. Camb. Engl.* **109**, 425–433.

23 King, Robert C. (1970) *Ovarian Development in Drosophila melanogaster* Academic Press, New York and London.

24 Deng WM & Bownes M (1998) Patterning and morphogenesis of the follicle cell epithelium during Drosophila oogenesis. *Int. J. Dev. Biol.* **42**, 541–552.

25 Ashburner M, Misra S, Roote J, Lewis SE, Blazej R, Davis T, Doyle C, Galle R, George R, Harris N, Hartzell G, Harvey D, Hong L, Houston K, Hoskins R, Johnson G, Martin C, Moshrefi A, Palazzolo M, Reese MG, Spradling A, Tsang G, Wan K, Whitelaw K & Celniker S (1999) An exploration of the sequence of a 2.9-Mb region of the genome of Drosophila melanogaster: the Adh region. *Genetics* **153**, 179–219.

26 Yan R, Thomas SE, Tsai J-H, Yamada Y & McKee BD (2010) SOLO: a meiotic protein required for centromere cohesion, coorientation, and SMC1 localization in Drosophila melanogaster. *J. Cell Biol.* **188**, 335–349.

27 Lasko PF & Ashburner M (1988) The product of the Drosophila gene vasa is very similar to eukaryotic initiation factor-4A. *Nature* **335**, 611–617.

28 Styhler S, Nakamura A, Swan A, Suter B & Lasko P (1998) vasa is required for GURKEN accumulation in the oocyte, and is involved in oocyte differentiation and germline cyst development. *Dev. Camb. Engl.* **125**, 1569–1578.

29 Tomancak P, Guichet A, Zavorszky P & Ephrussi A (1998) Oocyte polarity depends on regulation of gurken by Vasa. *Dev. Camb. Engl.* **125**, 1723–1732.

30 Johnstone O & Lasko P (2004) Interaction with eIF5B is essential for Vasa function during development. *Dev. Camb. Engl.* **131**, 4167–4178.

31 Dehghani M & Lasko P (2015) In vivo mapping of the functional regions of the DEAD-box helicase Vasa. *Biol. Open* **4**, 450–462.

32 Tinker R, Silver D & Montell DJ (1998) Requirement for the vasa RNA helicase in gurken mRNA localization. *Dev. Biol.* **199**, 1–10.

33 Ejsmont RK, Ahlfeld P, Pozniakovsky A, Stewart AF, Tomancak P & Sarov M (2011) Recombination-mediated genetic engineering of large genomic DNA transgenes. *Methods Mol. Biol. Clifton NJ* **772**, 445–458.

34 Gratz SJ, Rubinstein CD, Harrison MM, Wildonger J & O'Connor-Giles KM (2015) CRISPR-Cas9 Genome Editing in Drosophila. *Curr. Protoc. Mol. Biol. Ed. Frederick M Ausubel Al* **111**, 31.2.1-20.

35 Koch R, Ledermann R, Urwyler O, Heller M & Suter B (2009) Systematic functional analysis of Bicaudal-D serine phosphorylation and intragenic suppression of a female sterile allele of BicD. *PloS One* **4**, e4552.

36 Gratz SJ, Cummings AM, Nguyen JN, Hamm DC, Donohue LK, Harrison MM, Wildonger J & O'Connor-Giles KM (2013) Genome engineering of Drosophila with the CRISPR RNA-guided Cas9 nuclease. *Genetics* **194**, 1029–1035.

37 Gratz SJ, Ukken FP, Rubinstein CD, Thiede G, Donohue LK, Cummings AM & O'Connor-Giles KM (2014) Highly specific and efficient CRISPR/Cas9-catalyzed homology-directed repair in Drosophila. *Genetics* **196**, 961–971.

Figure legends

Figure 1. Degradation of the AID-tagged Nanos protein by the AID system. (A-C) Cuticle preparations from 24-hour-old embryos. Embryos are shown with anterior to the left. **(A)** A wild-type embryo, possessing a head, three thoracic, and eight abdominal segments. **(B)** A bicaudal embryo produced by a female expressing a mislocalized form of the Nanos protein (*AID:nos-bcd3'UTR*). Such embryos lack head structures and thoracic segments and form two abdomens consisting of 3-5 abdominal segments. As a result of this duplication, posterior terminal structures, such us the filzkörper (arrow), are located at both poles of the embryo. **(C)** Embryos laid by *AID:nos-bcd3'UTR; nosGal4VP16>UASpTIR1* females after auxin administration. Embryos show a suppressed bicaudal phenotype as they have an elongated shape with 6-8 abdominal segments and the filzkörper (arrow) has disappeared from the anterior side. **(D)** Time course of the auxin treatment. Females expressing the AID-tagged mislocalized form of Nanos and the TIR1 protein were crossed with w^{1118} males. Flies were fed with 1M auxin solution/yeast extract mixture. Auxin was withdrawn after one week, and flies were kept for an additional two days. Eggs were collected (N>100) daily, and the penetrance of cuticular phenotypes was determined.

Figure 2. Strategy for tagging the *vasa* gene by CRISPR/Cas9-induced homologous recombination. Guide RNA target sites (arrows) located in the last intron and downstream of the 3'UTR of the *vasa* gene. The donor construct was designed to insert the AID:EGFP tag right before the stop codon. The DsRed marker gene with the eye-specific 3XP3 promoter was introduced after the *vasa* locus into the intergenic region. LoxP sites allow the excision of the 3XP3 DsRed cassette by the Cre/loxP system. Introns and intergenic regions are shown as a line.

Figure 3. Expression pattern of the AID:EGFP-tagged (A-A') and wild-type (B) Vasa protein. (A) Vasa protein (green) in vasa:AID:EGFP homozygous flies was detected by EGFP fluorescence. **(A',B)** Vasa protein (red) in vasa:AID:EGFP homozygous flies **(A')** and in Oregon strain **(B)** was detected by staining with vasa antibody. DAPI labels the nuclei (blue). Adult ovarioles, adult germaria and early embryos are shown with anterior to the left. In ovarioles, Vasa protein accumulates around the nuclei of nurse cells and at the posterior pole of the developing oocyte. Scale bar represents 100µm. In germaria, Vasa protein is

expressed around the nuclei of germ cells. Scale bar represents 10μm. In early embryos, Vasa protein accumulates at the posterior pole. Scale bar represents 100μm.

Figure 4. Expression of AID:EGFP-tagged Vasa and the TIR1 protein in auxin-treated ovaries. *UASpTIR1:9xMyc* was expressed by *mat-tub-Gal4* (**A**) *NGT-Gal4* (**B**) and *nosGal4VP16* (**C-D**) drivers in the ovary of homozygous *vasa:AID:EGFP* flies. Ovarioles are shown with anterior to the left. The tagged Vasa protein is green. The Myc-tagged TIR1 protein (red) was stained with anti-Myc antibody. DAPI labels the nuclei (blue). Scale bar represents 100μm. (**A-C**) Flies were fed with 1M auxin solution/yeast extract mixture for three days, and then their ovaries were stained. Inset in **B** shows magnified view of the germarium. Scale bar represents 20μm. (**D**) Flies were fed with 1M auxin solution/yeast extract mixture for three days, and their ovaries were stained after two days of auxin withdawal.

Figure 5. Western blot analysis of the Vasa:AID:EGFP protein in the ovary of *vasa:AID:EGFP, nosGal4VP16>UASpTIR1* females. Flies were fed with 1M auxin solution/yeast extract mixture for three days. After the treatment, auxin was withdrawn and flies were kept for additional two days. Control flies of the same age and without auxin treatment were also examined. The Vasa:AID:EGFP protein was labeled with anti-GFP antibody; β-tubulin served as a loading control.

Figure 6. Cuticular phenotype of a first instar larva produced by *vasa:AID:EGFP, nosGal4VP16>UASpTIR1* females before (A) and after (B) auxin treatment. Samples were collected after 24 hours of egg laying. Larvae are shown with anterior to the left. **A**. Larva shows wild-type phenotype with head, three thoracic, and eight abdominal segments. **B**. Larva lacks abdominal segments, showing the classical posterior vasa phenotype.

Figure 7. Expression of the Gurken protein in the ovary of the *vasa:AID:EGFP; mat-tub-Gal4>UASpTIR1* females. Ovarioles are shown with anterior to the left. Flies were fed with yeast extract (**A**) or with 1M auxin solution/yeast extract mixture (**B**) for three days, and then their ovaries were stained. The tagged Vasa protein is green. The Gurken protein (red) was stained with anti-Gurken antibody. DAPI labels the nuclei (blue). Scale bar represents 100 μm. Gurken is located at the posterior pole of the oocyte (arrows) in the early stage egg

chambers. During the mid-oogenesis Gurken is found at the dorsal-anterior corner of the oocyte (arrowhead).

Figure 8. Reversible depletion of the AID:EGFP-tagged Vasa protein by the AID system. *vasa:AID:EGFP, nosGal4VP16>UASpTIR1* females (**A**) and *vasa:AID:EGFP, UASpTIR1* females (**B**) were crossed with w^{1118} males and fed with 1M auxin solution/yeast extract mixture for four days. After the treatment, auxin was withdrawn, and the flies were kept for an additional two days. Eggs were collected (N>100) daily, and the penetrance of cuticular phenotypes was determined. (**C**) Western blot analysis of the Vasa protein in laid eggs of auxin treated vasa:AID:EGFP, nosGal4VP16>UASpTIR1 females. 0-2-hour old eggs were collected daily. The Vasa:AID:EGFP protein was labeled with anti-GFP antibody; β-tubulin served as a loading control.

Figure 9. Auxin induces protein degradation in a concentration-dependent manner. *vasa:AID:EGFP, nosGal4VP16>UASpTIR1* females were crossed with w^{1118} males. Flies were fed with auxin solution/yeast extract mixture, prepared in increasing concentrations (0-4M) of auxin. (**A**) Eggs were collected (N>100) after three days, and the penetrance of cuticular phenotypes was determined. (**B**) Western blot analysis of the Vasa protein in laid eggs. 0-2-hour old eggs were collected daily. The Vasa:AID:EGFP protein was labeled with anti-GFP antibody; β-tubulin served as a loading control.

Figure 10. Partial Vasa degradation by low auxin concentrations results in a grandchildless phenotype. *vasa:AID:EGFP, nosGal4VP16>UASpTIR1* females were crossed with w^{1118} males and fed with auxin (0-250 mM)/yeast extract mixture for three days. Gonads were dissected from female (**A**) and male (**B**) adult progeny (N>50) of the auxin-treated flies. Penetrance of flies with normal gonads and flies where one (mosaic) or both gonads showed agametic phenotype was determined.

Figure 11. Auxin analogues are able to activate the AID system. *vasa:AID:EGFP, nosGal4VP16>UASpTIR1* females were crossed with w^{1118} males and fed with yeast paste prepared with 25 mM and 200 mM 2,4-dichlorophenoxyacetic acid (2,4-D) and 1-naphthaleneacetic acid (1-NAA). After three days, the laid eggs were collected (N>100), and the penetrance of cuticular phenotypes was determined.
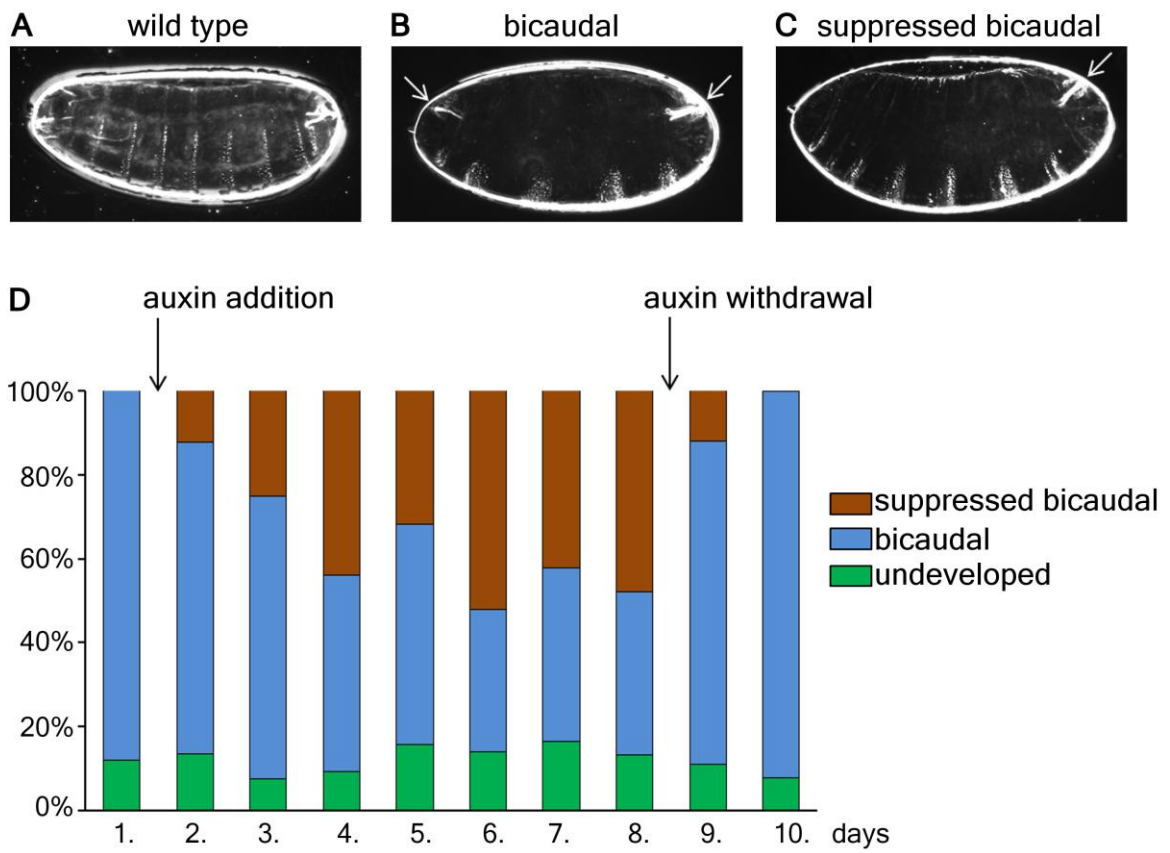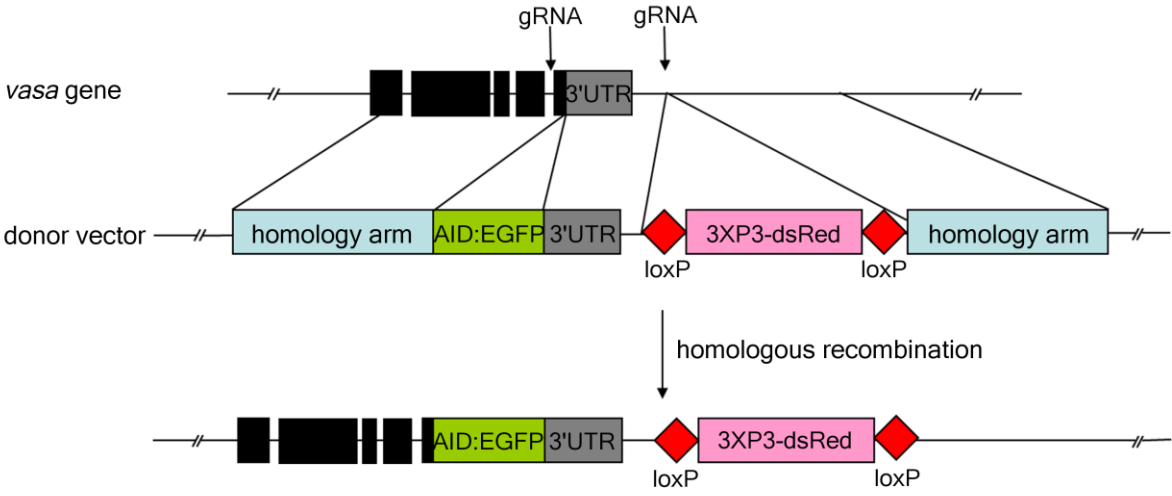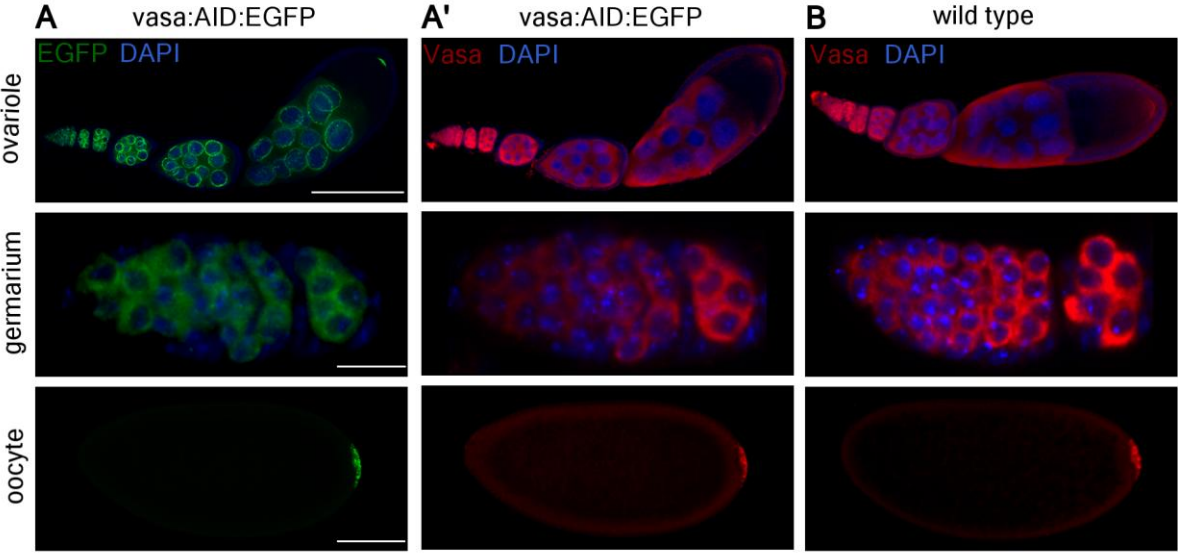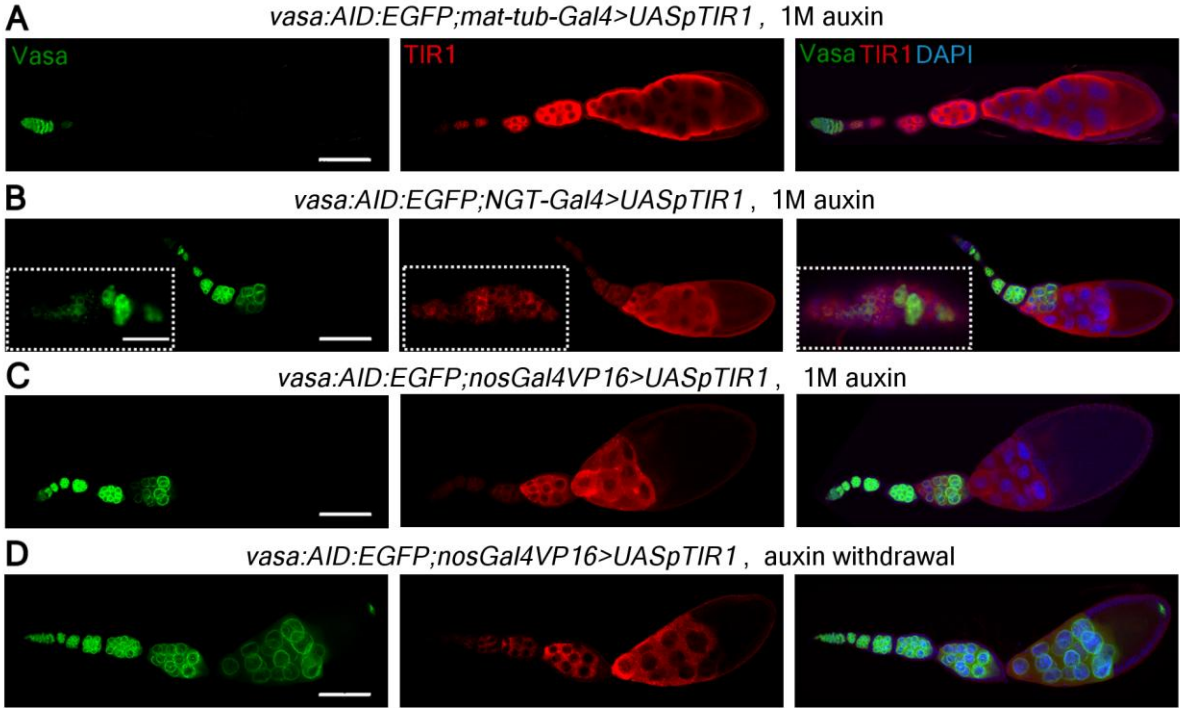
Figure 1

A wild type   B bicaudal   C suppressed bicaudal

D

Figure 2

Figure 3

Figure 4

A   *vasa:AID:EGFP;mat-tub-Gal4>UASpTIR1 ,* 1M auxin

Vasa   TIR1   Vasa TIR1 DAPI

B   *vasa:AID:EGFP;NGT-Gal4>UASpTIR1 ,* 1M auxin

C   *vasa:AID:EGFP;nosGal4VP16>UASpTIR1 ,* 1M auxin

D   *vasa:AID:EGFP;nosGal4VP16>UASpTIR1 ,* auxin withdrawal

Figure 5

vasa:AID:EGFP;nosGal4VP16>UASpTIR1
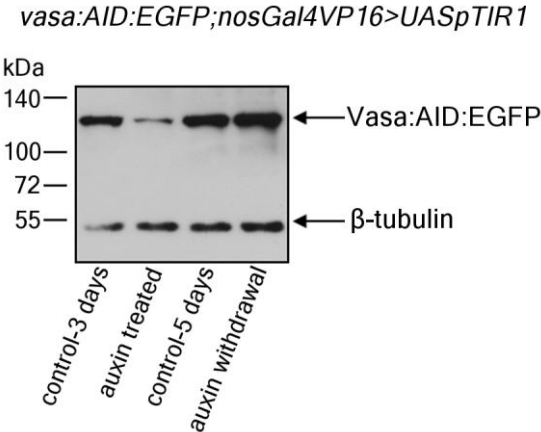
Figure 6

A *vasa:AID:EGFP;nosGal4VP16>UASpTIR1*
Control
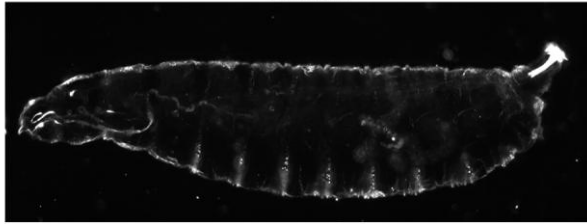
B *vasa:AID:EGFP;nosGal4VP16>UASpTIR1*
1M auxin
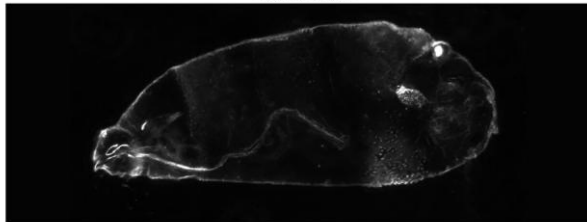
Figure 7
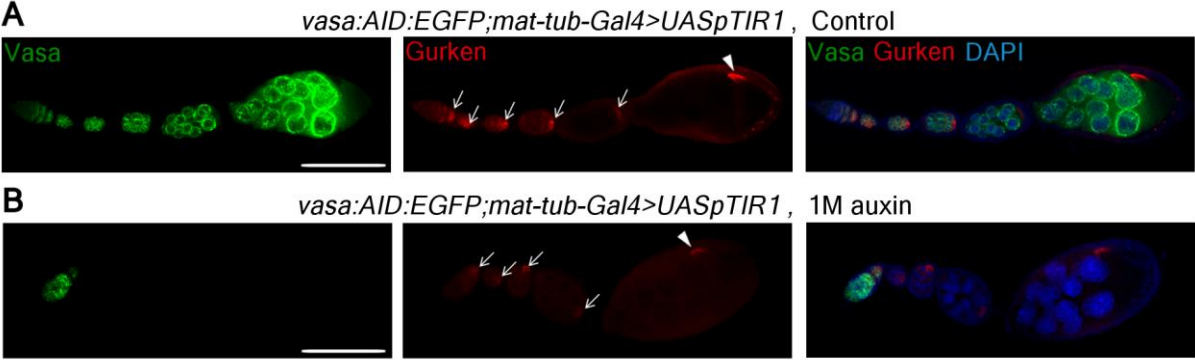
Figure 8

A *vasa:AID:EGFP;nosGal4VP16>UASpTIR1*
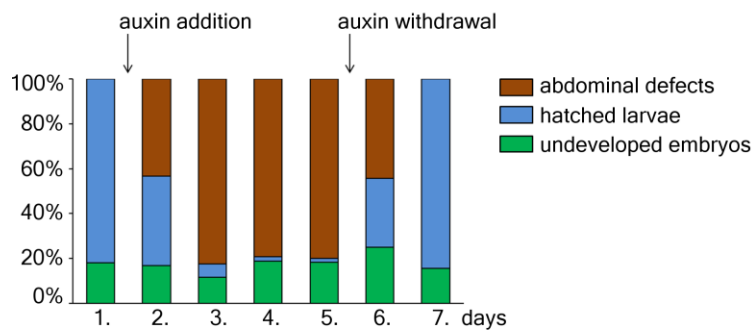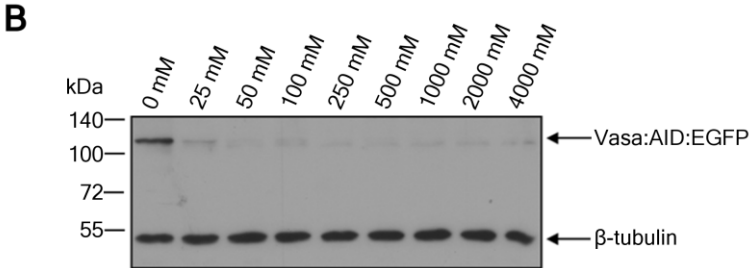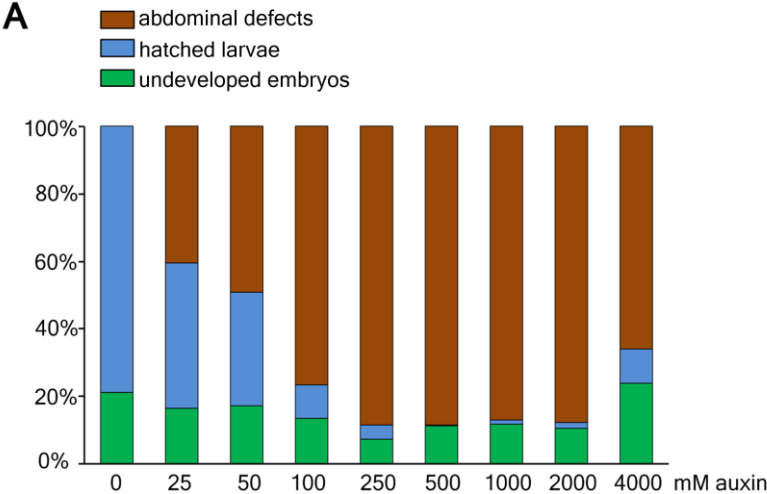

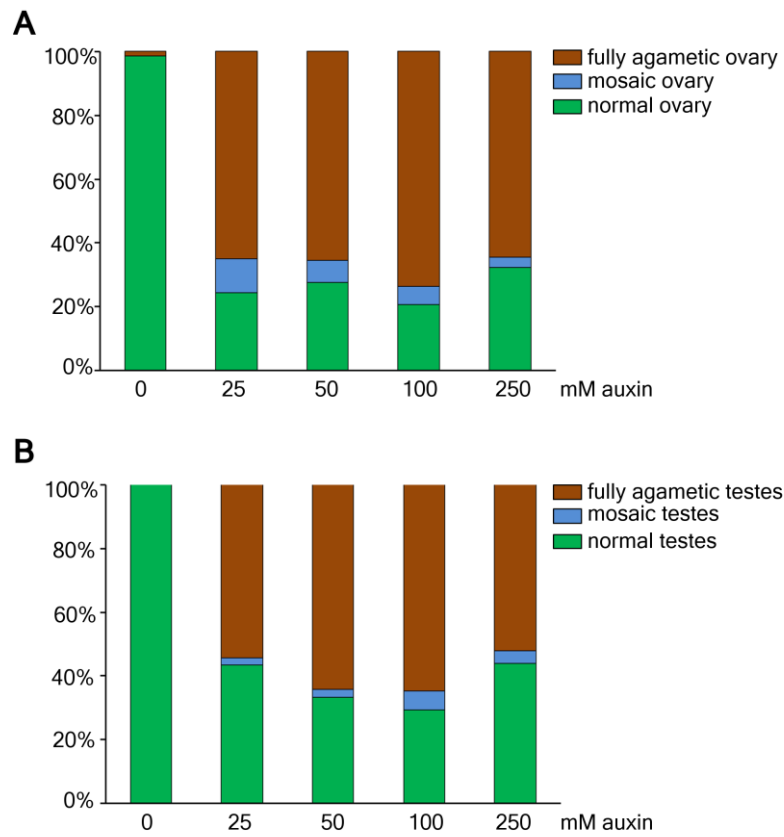**B** *vasa:AID:EGFP;UASpTIR1*
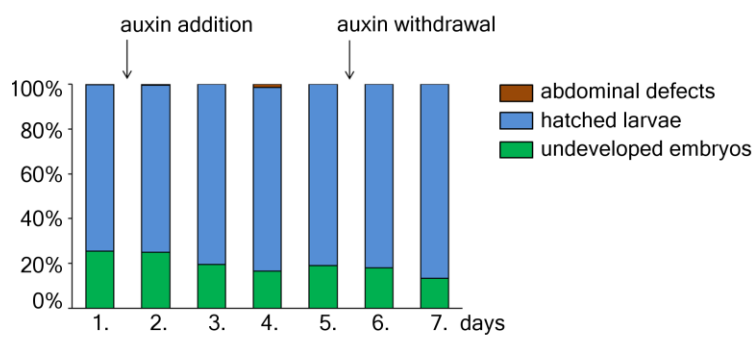
C *vasa:AID:EGFP;nosGal4VP16>UASpTIR1*
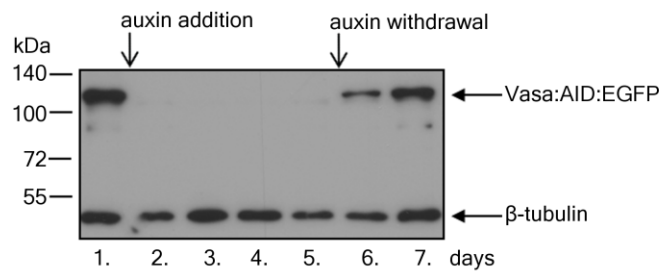
Figure 9

Figure 10

Figure 11